

# EFFICIENCY MEASUREMENT OF A 3-PHASE INVERTER FOR A BLDC MOTOR

## Products:

- ▶ R&S®RTM3004
  - ▶ R&S®RT-ZHD07
  - ▶ R&S®RT-ZC10B
  - ▶ R&S®RT-ZF20
- ▶ R&S®NGP814

Johannes Ungar (TUM Hyperloop), Faruk Centinkaya (TUM Hyperloop), Marcus Sonst (R&S) | GFM360 |  
Version 0e | 04.2021

<http://www.rohde-schwarz.com/appnote/GFM360>

# Contents

<b>1</b>	<b>Overview</b> .....	<b>3</b>
<b>2</b>	<b>Introduction</b> .....	<b>4</b>
<b>3</b>	<b>Motor and Control</b> .....	<b>5</b>
3.1	Brushless Motor .....	5
3.1.1	Differences Between PMSM and BLDC Motor .....	6
3.2	Control Methods of Brushless Motors .....	6
3.2.1	Trapezoidal Control .....	7
3.2.2	Sinusoidal Control .....	9
3.2.3	Field Oriented Control (FOC) .....	9
3.2.4	Sensorless Control .....	9
<b>4</b>	<b>Theory of Power Measurement and Drive Inverter Efficiency</b> .....	<b>10</b>
4.1	Efficiency of the Drive Inverter .....	10
4.2	Input Power Measurement .....	10
4.3	Output Power Measurement .....	11
4.3.1	Blondel's Theorem .....	11
4.3.2	Two-Wattmeter Method .....	11
<b>5</b>	<b>Measurement Equipment and Test Setup</b> .....	<b>13</b>
5.1	Motor Test Bench .....	13
5.2	Oscilloscope .....	14
5.3	Probes and Tools .....	14
5.4	Power Supply .....	14
<b>6</b>	<b>Measurement Preparation</b> .....	<b>15</b>
6.1	Demagnetization .....	15
6.2	Zero adjust .....	15
6.3	Deskew .....	15
<b>7</b>	<b>Measurement Evaluation</b> .....	<b>17</b>
7.1.1	DC-Bus Measurements .....	17
7.1.2	Inverter Measurements .....	18
7.1.3	Inverter Efficiency.....	20
<b>8</b>	<b>Conclusion</b> .....	<b>21</b>
<b>9</b>	<b>Literature</b> .....	<b>22</b>
<b>10</b>	<b>Ordering Information</b> .....	<b>23</b>

# 1 Overview

This application note introduces the reader to the SpaceX Hyperloop Pod Competition project and their special demands for the electrical drive train. Common motor technology like brushless motors and their typical control methods widely used in the industry are also discussed within this document.

However, the main focus of this paper is a demonstration of a power measurement method of a three-phase inverter by means of a 4-channel oscilloscope. Not only the theory of the power measurement is presented but also the conducted measurement is presented including tips and tricks to obtain the best measurement results.

The measurement solution provided by Rohde & Schwarz was mandatory for the TUM Hyperloop team to overcome challenges in optimization of the electrical drive train used in the SpaceX Hyperloop Pod Competition project.

Many thanks to Mr. Johannes Ungar and Faruk Centinkaya (TUM Hyperloop) for contributing significantly to this application note. By combining their expertise in electrical drive trains used in the Hyperloop Project and with a Test & Measurement solution from Rohde & Schwarz, we have achieved synergies that will be beneficial for any design and test engineers in the industry.

## 2 Introduction

The Hyperloop team from the Technical University of Munich (TUM) participated in four editions of the “SpaceX Hyperloop Pod Competition”. The main objective of the competition was to accelerate the development of functional Hyperloop prototypes and to encourage student innovation. Therefore, a 1.2 km long vacuum steel tube was built next to the SpaceX headquarters in Hawthorne, California. The competition was dominated by the student team TUM Hyperloop from the Technical University of Munich (TUM), winning four consecutive times with the fastest pod.

To improve the performance in the last competition, the TUM Hyperloop team focused their efforts on the optimization of the electric drivetrain through thorough testing and simulations. One part of this testing program, and main objective in this application note, is the power efficiency measurement of the three-phase inverter, which converts the DC-input from the battery to a three-phase output for the motor.

A specific motor test bench in the lab was used to evaluate the proposed power-efficiency measurement concept. However, the motor and motor drive system which were examined in this application note are different than those used in the Hyperloop Pod. They are rated for much lower power levels and allow a much safer operation in a standard laboratory environment. The differences between the Hyperloop Pod IV (high power system) and the motor test bench used in the laboratory are shown in Table 2-1. Nevertheless, the measurement method is also applicable for the real high-power system.

Parameters	Hyperloop Pod IV	Motor Test Bench
Motor Control	Trapezoidal Control	Field-Oriented Control
Motor	PMSM Inrunner Motor	BLDC Outrunner Motor
Maximum Speed Of Motor	50000 rpm	4000 rpm
Peak Torque	7.5 Nm	Not Measured
Maximum Voltage	120 V	24 V
Maximum Phase Current	500 A	40 A
Peak Power	40 kW	600 W

Table 2-1: Key Parameters of the Electrical Drive Train.

The two-wattmeter method was chosen to measure the active power supplied to the motor. This method, also called Aron insertion, can be used in three-wire, three-phase systems and only requires two wattmeters to measure the total active power of the system. The DC input power of the inverter was supplied and measured by the 4-channel power supply R&S®NGP-814.

The three-phase power signals were measured with two R&S® RT-ZHD07 voltage differential probes and two R&S®RT-ZC10B current probes. The 4-channel digital oscilloscope R&S®RTM-3004 with its built-in “Math-function” was used to analyze the signals and to perform the power calculations. The tested motor was loaded by means of a six-pulse bridge rectifier circuit which was connected to an electronically controlled DC-load. Hereby, the motor and its drive inverter can be examined for different load conditions. Moreover, the working conditions can be held stationary during the measurement process.

# 3 Motor and Control

## 3.1 Brushless Motor

A brushless motor or generator has no mechanical contacting parts like brushes or slip-rings to transfer electrical energy from a stationary to a moving part [1]. Several types of machines satisfy this basic definition including induction motors (asynchronous), switched reluctance machines and synchronous machines. The primary interest in this application note is on the brushless DC (BLDC) motor, also referred to as electronically commutated motor. Commonly the BLDC motor structure is also known as a Permanent Magnet Synchronous Motor (PMSM) with surface mounted magnets and concentrated windings [2, p. 47]. However, in some industries the term BLDC is more established.

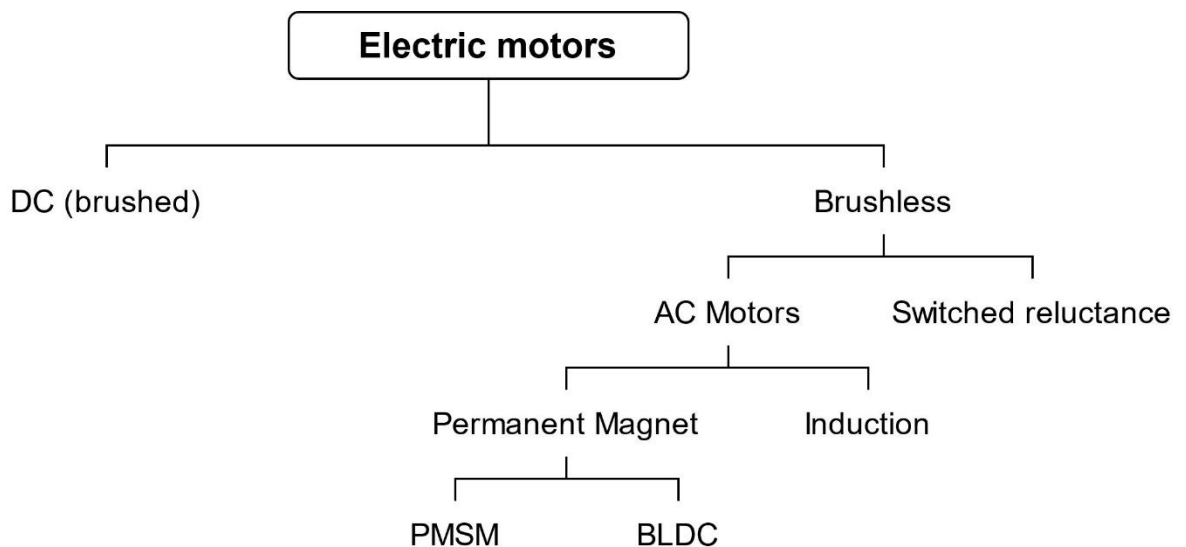


Figure 3-1: Classification of PMSM and BLDC Motors [3].

Figure 3-1 shows a typical classification of electric motors for a particular application in the fractional to 20 kW range [3]. Reasons why brushless motors are chosen in favor of brushed motors include robustness, lower maintenance, and higher torque and speed bandwidths. Furthermore, mechanical commutators are severely limiting the maximum speed and overcurrent capabilities which is why a brushless motor was chosen for the Hyperloop pod.

### 3.1.1 Differences Between PMSM and BLDC Motor

As stated in the introductory chapter a PMSM was used in the Hyperloop Pod. BLDC motors would also have been a viable solution. However, the most powerful motor available on the market which met the requirements of the high-speed pod was a PMSM. Since, in this application note a BLDC motor with much less power was examined it is crucial to understand the fundamental differences between the two motor types.

The PMSM has a sinusoidal back EMF (Electromotive Force), whereas the BLDC motor is characterized by a trapezoidal back EMF [3]. Both have a permanent magnet rotor, but the difference is in the winding arrangement of the stator and shaping of the magnets. Sinusoidal stator currents are needed to produce a steady torque in the PMSM, whereas rectangular-shaped currents are needed to produce a steady torque in the BLDC motor. It is this difference that has numerous ramifications both in the behavior of the motor drive and in the structure of the control algorithms and circuitry [3].

## 3.2 Control Methods of Brushless Motors

According to [2] the most common control modes, for brushless DC motors, are

- ▶ Trapezoidal Control or Block Commutation,
- ▶ Sinusoidal Control,
- ▶ Field-Oriented Control (FOC),
- ▶ Sensorless Control,

whereby sensorless control is just indicating that no sensor equipment is used to determine the rotor position. Instead, the rotor position can be estimated by evaluating the back-EMF of the motor (see chapter Sensorless Control). In general, all control algorithms designed for synchronous machines with concentrated windings can also be applied to BLDC motors [2].

In Table 3-1, the different control methods used in the Hyperloop Pod and the motor test bench are shown. As will be described later, a sensorless control was not possible in the propulsion system of the Hyperloop Pod. The large initial torque on the drive wheel made it impossible to achieve stable commutation of the motor. However, in the motor test bench used in this application note, the load on the motor can be varied freely, which allows a “no-load” startup to attain the necessary motor speed for sensorless control.

Parameters	Hyperloop Pod IV	Motor Test Bench
Control method	Trapezoidal Control	Field-Oriented Control
Rotor position sensing	3 Hall Sensors	Sensorless (derived from back-EMF of motor)
Motor back EMF	Sinusoidal	Trapezoidal

Table 3-1: Control Methods in the Hyperloop Pod IV and the Motor Test Bench.

### 3.2.1 Trapezoidal Control

Trapezoidal control is one of the most common and simplest algorithms to drive BLDC motors [2]. However, compared to self-commutating brushed motors, BLDC motors require sophisticated electronics and are significantly more complex to control since they are not self-commutating [4].

The BLDC motor in its most common form has a rotor with permanent magnets and a stator with windings as illustrated in Figure 3-2.

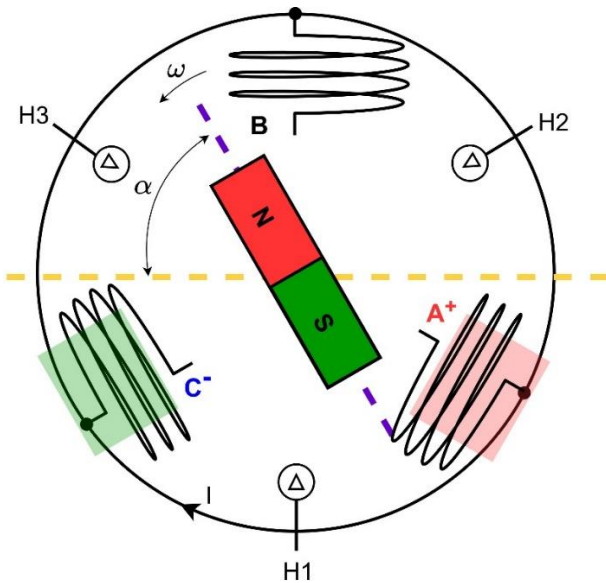


Figure 3-2: Winding arrangement and rotor alignment for a three-phase BLDC motor.

No parts in direct mechanical contact such as brushes or commutators are present. Instead, the windings are connected to an electronic control system which replaces the function of the commutator. In trapezoidal control for three-phase machines, also known as six-step control, voltage is applied to only two of the three stator windings at one time [5]. The windings are energized in a certain pattern leading to a rotating magnetic field in the stator. Refer to Figure 3-2 for the required voltage waveforms. The rotor magnet follows this motion and the stator windings are switched just as the magnetic field of the rotor starts aligning with the magnetic field of the stator.

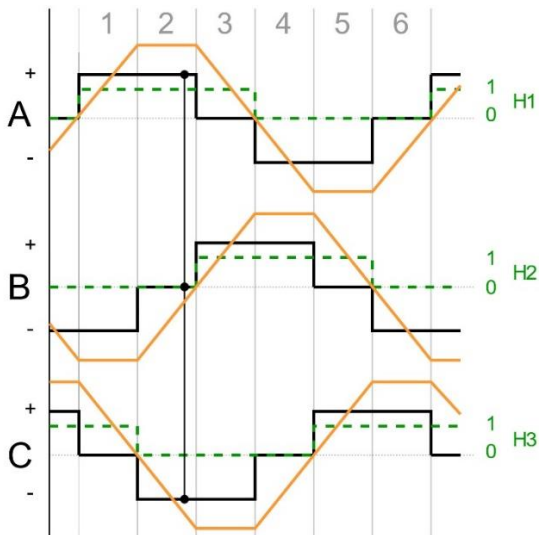


Figure 3-3: Corresponding Hall-sensor signals (green), voltage waveforms (black) and back EMFs (orange) of phase A, B and C.

The three-phase winding of the stator can be connected in six different ways → six commutation steps. The motor in Figure 3-2 is shown at the end of commutation step 2 where coil A and C are energized. The angle between the magnetic field of the rotor (— — —) and the magnetic field of the stator (— — —) is expressed with  $\alpha$ . For maximum torque  $\alpha$  must be  $90^\circ$ .

The right switching time is indicated by three rotor position sensors (Hall sensor or encoder). As soon as the rotor passes the hall sensor, the controller switches the DC voltage to the next phase “A”, “B” or “C” (refer to Figure 3-3). Therefore, the control algorithm is rather simple and requires only a lightweight microcontroller for algorithmic execution. As shown in Figure 3-3 the voltage has a rectangular shape (A, B, C). By the design of the BLDC motor it generates a trapezoidal back EMF shape. The measured back EMF signal of one phase of the investigated BLDC motor is shown in Figure 3-4. It clearly resembles the trapezoidal signal shape as shown in Figure 3-3.



Figure 3-4: Trapezoidal Back EMF measured in one Phase of the BLDC motor.

Torque is produced by the interaction of the magnetic field in the stator and the rotor. Maximum torque is produced when these two fields are aligned at  $90^\circ$  to each other [4]. However, since the magnetic field in the stator remains stationary in each commutation step while the rotor is constantly moving it is impossible to have a perfect  $90^\circ$ -alignment for all times. Hence, the torque is never perfectly constant leading to torque ripples, vibration, noise and an overall poorer performance compared to other algorithms.

### 3.2.2 Sinusoidal Control

Sinusoidal control is also known as voltage-over-frequency commutation and overcomes many of the issues caused by trapezoidal control. It supplies a smoothly (sinusoidal) varying current to the three excitation windings, and, therefore, reduces the torque ripples. [2]

However, to convert DC current into smoothly varying phase currents complex control electronics, known as variable frequency drives (VSDs), are required [5]. Moreover, the sinusoidal commutation ideally needs a higher resolution system for determining the rotor position. Normally, this consists of an optical or magnetic encoder that determines the position of the rotor with sufficient precision at all times. [2]

### 3.2.3 Field Oriented Control (FOC)

Field oriented control (FOC) combines the advantages of trapezoidal and sinusoidal control providing smooth operation at slow speeds as well as an efficient operation at high speeds [4]. It guarantees superior efficiency values even during transient operation when compared to all other control techniques [2].

Main objective of FOC is to keep the magnetic field of the rotor and the stator perfectly aligned with an angle  $\alpha = 90^\circ$  (refer to Figure 3-2). Unlike in trapezoidal control where the magnetic flux vector of the stator can only be oriented in six discrete positions (six commutation steps), the stator flux vector in FOC can continuously move like the rotor. This can only be achieved by simultaneously energizing all three phases with continuously varying currents, making FOC much more complex than trapezoidal control.

The main characteristic of FOC, or also called vector control, is the identification of the three-phase stator current system as an orthogonal two-phase system. Hereby, mathematical transformations from the three-phase system to a two-phase system are needed. The two parameters flux linkage and torque form the current space vector which can be controlled independently in almost any load condition [2].

### 3.2.4 Sensorless Control

Sensorless control methods utilize the back EMF of the motor to determine the rotor position and does not require any hall sensors or optical encoders. The back EMF as shown in Figure 3-3 can be measured and used to compute the switching signals of all phases [2].

Main disadvantage of sensorless control is that no information on the rotor position is available when idle, thus a special startup method is required. This is especially problematic when a large initial torque is present on the motor shaft so that the wheel cannot turn freely.

# 4 Theory of Power Measurement and Drive Inverter Efficiency

The drive inverter is supplied with DC power from the power supply and generates a three-phase signal (A, B, C) for the motor. Input power  $P_{in}$  and output power  $P_{out}$  of the drive inverter needs to be measured in order to compute its power efficiency  $\eta$  (refer to Figure 4-1). Two wattmeters W1 and W2 are used to measure the three-phase output power of the drive inverter.

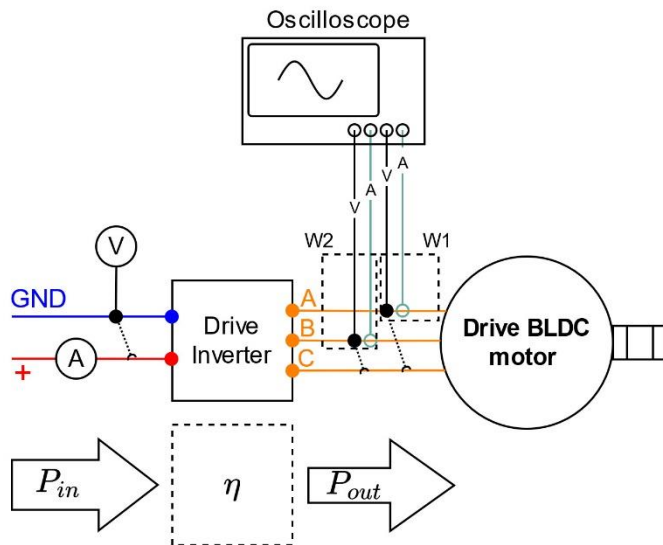


Figure 4-1: Power Efficiency Measurement of the Drive Inverter.

## 4.1 Efficiency of the Drive Inverter

The electrical efficiency of the drive inverter system can be calculated based on the ratio between its output and input power (refer to Figure 4-1).

$$\eta = \frac{P_{out}}{P_{in}} \quad (1)$$

## 4.2 Input Power Measurement

The DC input power of the drive inverter can be measured with the product of voltage and current obtained by means of a volt-ampere measurement.

$$P_{in} = V * I \quad (2)$$

In case of the R&S®NGP814 the power values are directly measured by the power supply itself and individually displayed for each channel.

## 4.3 Output Power Measurement

### 4.3.1 Blondel's Theorem

By utilizing Blondel's theorem [6], the two-wattmeter method reduces the number of required channels to measure the active power of a three-phase system from six to four. In essence, Blondel's theorem states that to correctly measure the total system power, it is permissible to use one less wattmeter than current-carrying conductors [7]. Furthermore, it states that the common point for the voltage measurement is the conductor without a wattmeter current connection. The circuit can be operated at any power factor or condition of current or voltage unbalance [7].

Hence, the two-wattmeter method is not only helpful to save valuable inputs on the measurement instruments, but can also be used for motors where a neutral point is not available e.g. a delta winding or an inaccessible neutral in a star winding [5].

### 4.3.2 Two-Wattmeter Method

In case of a three-phase 3-wire system as it was used in the scope of this work, a two-wattmeter method can be realized by measuring two line-line voltages, A and B, to a common line reference C, and two-line current measurements in A and B (refer to Figure 4-2). It is important that the current is measured in the lines which are not used as the common line reference for the voltage measurements.

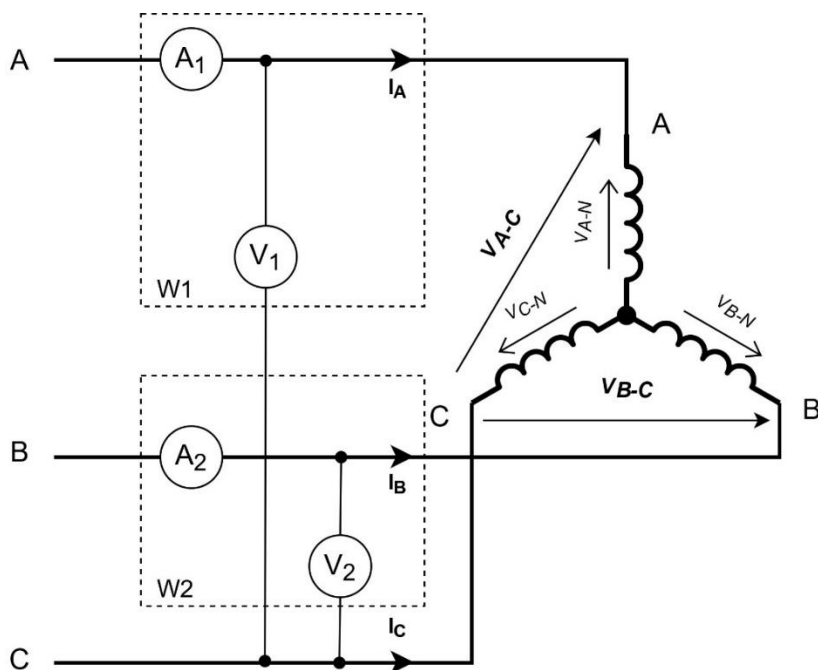


Figure 4-2: Three-phase, three-wire WYE connected system.

The total active power for the two-wattmeter method is defined as

$$\Sigma P = P_{W1} + P_{W2} \quad (3)$$

$$\Sigma P = V_1 A_1 + V_2 A_2 \quad (4)$$

This can be rewritten in the following way to obtain an expression solely dependent on the line-neutral voltages

$$\Sigma P = (V_{A-N} - V_{C-N}) I_A + (V_{B-N} - V_{C-N}) I_B \quad (5)$$

$$\Sigma P = V_{A-N} I_A + V_{B-N} I_B - V_{C-N} (I_A + I_B) \quad (6)$$

Since according to Kirchhoff's law  $I_A + I_B + I_C = 0$  we get the well-known expression for the total instantaneous power of a three-phase system

$$\Sigma P = V_{A-N} I_A + V_{B-N} I_B + V_{C-N} I_C \quad (7)$$

which corresponds to a measurement with the three-wattmeter method. Hence, it is proven that the measurement of two line-line voltages and two line currents are sufficient in order to determine the total active power of a three-phase system.

It is important to note that the calculated per-phase power values in the two-wattmeter method do not represent the coil powers, though they will correctly sum to the total three phase power [5].

# 5 Measurement Equipment and Test Setup

## 5.1 Motor Test Bench

The motor test setup shown in Figure 5-1 consists of two rigidly coupled BLDC motors. The drive inverter is supplied with electric energy from a DC power supply, which is converted into three-phase electric power to drive the BLDC motor. The mechanical rotation of the drive BLDC motor is transferred to the load BLDC motor with a rigid coupling. Hereby, the load BLDC motor starts to generate electric power which can be used to vary the load conditions on the drive motor by using a DC electronic load. In order to convert the three-phase AC to DC, a full bridge rectifier circuit and capacitor block connected to the load side of the BLDC motor is used.

Equipment used in the motor test bench:

- ▶ 2x BLDC motor (600W, 24V, 4000 rpm): 8-pole outrunner motor with surface mounted PMs and concentrated windings.
- ▶ Drive inverter (object to be measured): An off-the shelf electronic speed controller (ESC) rated for 60V and 80A continuous featuring FOC-control method. The exact electronic architecture is not known nor its power efficiency values.
- ▶ Three-phase full bridge rectifier circuit: The power stage from an electronic speed controller rated for 400 A continuous current and 60 V was used as a rectifier circuit.
- ▶ DC electronic load: H&H PLI6406
- ▶ 4-channel DC power supply R&S®NGP814

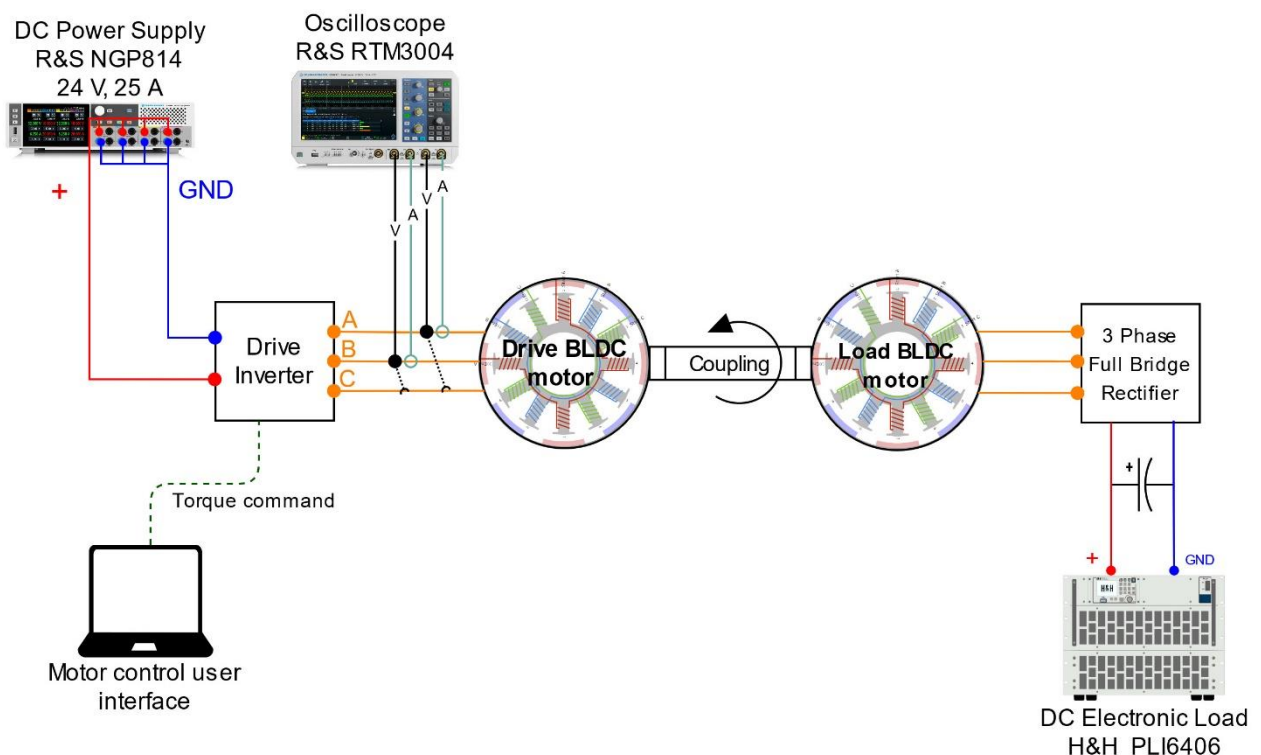


Figure 5-1: Motor Test Bench Setup.

## 5.2 Oscilloscope

A minimum 4-channel 70 MHz oscilloscope is required for this application. Preferably models with new Rohde & Schwarz probe interface. R&S®RTM3004 was used in this application.

## 5.3 Probes and Tools

Probes required for this application:

- ▶ 2x current probes, enough current range based on motor specifications, R&S®RT-ZC10B, or similar
- ▶ 2x high voltage differential probes, R&S®RT-ZHD07, or similar
- ▶ R&S®RT-ZF20 power deskew fixture

## 5.4 Power Supply

A power supply is required which can provide stable current and voltage level for dynamic inverter test. Data logging, wide power levels essential for our inverter input power measurement. R&S®NGP814 used on this application base on maximum 800W output power and multiple channel option which can be connected in series or parallel for up to 192 V or 60 A.

# 6 Measurement Preparation

Before starting any measurement all the test equipment needs to run at least 30 minutes early at room temperature to warm up the devices. In this way, you can get specified device tolerances.

However, the power measurement required a current probe that's why 3 additional steps need to be done.

## 6.1 Demagnetization

- ▶ Make sure that there is no conductor inside of the current probe aperture. Wrong use can damage the sensor.
- ▶ Close the probe clamp and press the slider on the sensor head until you see the lock indicator.
- ▶ Connect the R&S®RT-ZC10B or similar current probe as described in the current probe manual.
- ▶ Normally, when you connect current probes that have a R&S probe interface, the oscilloscope automatically demagnetizes the probe. In case you need to demagnetize again, you can press channel probe setup and then tap "DeGauss".

## 6.2 Zero adjust

- ▶ After demagnetization always carry out a zero adjustment
- ▶ Locate the current probe away from any conductor.
- ▶ Select the proper vertical scale for your application and then start to adjust the current level until the specified zero error level of the probe is reached.

Tip: On R&S®RTO/RTE/RTP instruments, you can tap "Detect AutoZero" to demagnetize and adjust to zero position in one step.

Tip: Tap "Save to probe" to store the "Zero adjust" value in the probe box. If you connect the probe to another channel or to another R&S oscilloscope, the value is read out again.

## 6.3 Deskew

Deskewing means to align the edges of two waveforms output by two different probes. The R&S®RT-ZF20 power deskew fixture is a tool to align the time delay (skew) of any combination of voltage and current probes. Deskewing is essential for power measurements. Preferably, this should be carried out before every measurement.

1. Connect a current probe to the oscilloscope,
2. Connect a voltage probe to another channel
3. Select proper loop for both probe base on deskew fixture user manual [R&S®RT-ZF20]
4. Set the horizontal scale
  - Large loop: 100 ns/div (for probes <20 MHz)
  - Small loop, rising edge: 20 ns/div (for probes <200 MHz)
  - Small loop, falling edge: 1 ns/div (for fast probes)
5. Set vertical scale

- ▶ For current probe: Large loop, R&S®RT-ZC05B/10/10B: 200 mA/div  
Small loop, R&S®RT-ZC15B/20/20B/30: 50 mA/div
  
- ▶ For voltage probe: Large loop: 1 V/div  
Small loop: 500 mV/div
  
- ▶ Set up trigger level. For more information please refer to the R&S®RT-ZF20 user manual.

# 7 Measurement Evaluation

## 7.1.1 DC-Bus Measurements

Each channel of the R&S®NGP-814 power supply is able to provide a maximum power of 200 W. To increase power and current output all 4 channels of the power supply were connected in parallel, which gives a maximum current output of 60 A. The R&S®NGP-800 power supply series comes with separate voltage and current meters on each output. Voltage, current and power values are individually displayed on the LED-screen for each output channel. Once a steady state was achieved on the motor test bench the output power values of each channel were added up to get the overall DC input power of the drive inverter.

$$P_{in} = P_{C1} + P_{C2} + P_{C3} + P_{C4} \quad (8)$$

In the example shown in Figure 3-1 the total DC power input to the drive inverter for a 30 A load test with 1250 rpm was  $P_{in} = 182.85 \text{ W}$ .

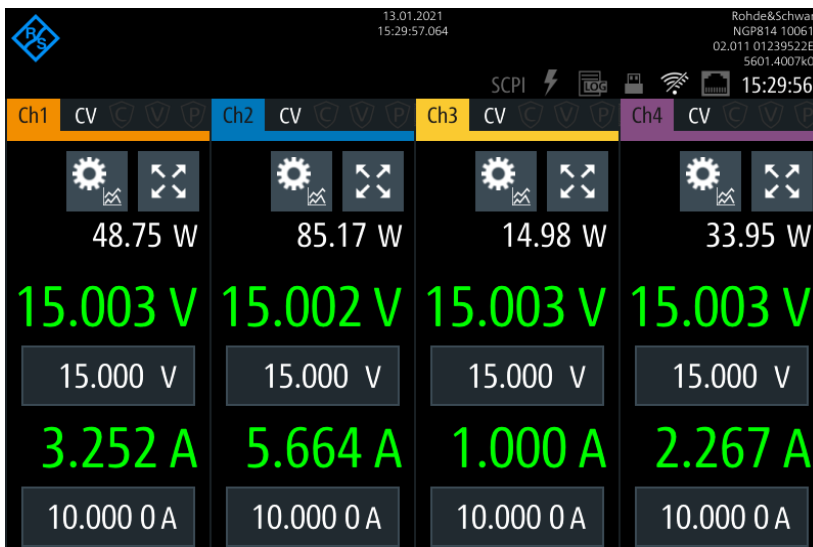


Figure 7-1: Input Power Values of the Power Supply.

## 7.1.2 Inverter Measurements

The output power measurement of the drive inverter was conducted with the two-wattmeter method as described in Chapter 2. Figure 7-2 shows the captured voltage and current signals for a 30 A load test with 1250 rpm. This means that the electronic DC-load, which is connected to the load motor was set to a constant value of 30 A.

The current waveforms on channel 1 and channel 2 are shown in yellow and green, and are very close to a sinusoidal shape. Current peak values are around 38 A. The sinusoidal shape is mainly due to the field-oriented control method. The square-shaped voltage waveforms on C3 and C4 are shown in orange and purple. Maximum voltage is 15 V as it was set on the power supply (refer to Figure 7-1).

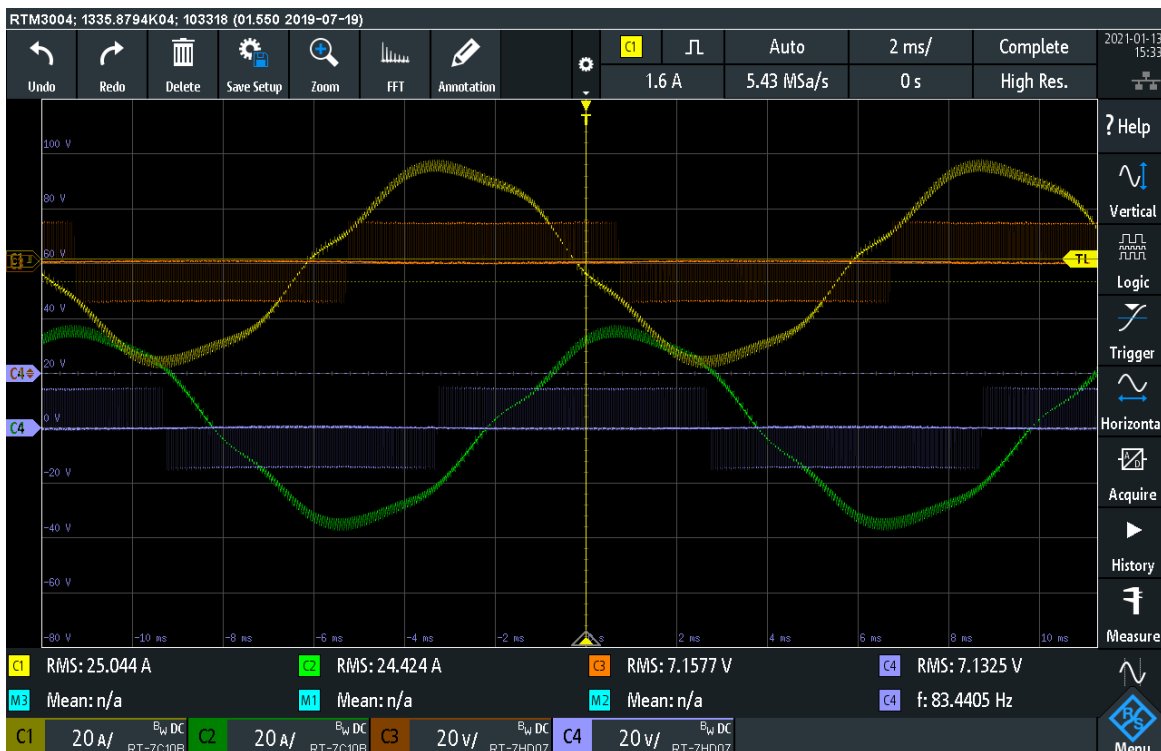


Figure 7-2: Phase Voltage and Currents.

To obtain the total active three-phase power, Equation (4) has to be applied on the voltage and current signals shown in Figure 7-2. On the R&S®RTM3004 this can be done by math waveforms. A math waveform is a waveform that is calculated from one or two analog channels, a constant, or another math waveform using several predefined operations. For the two-wattmeter method three equations need to be defined (refer to Figure 7-3):

- ▶ Multiplication of the first voltage and current waveform:  $C1 \times C3 \rightarrow M1$
- ▶ Multiplication of the second voltage and current waveform:  $C2 \times C4 \rightarrow M2$
- ▶ Addition of the precomputed math waveforms M1 and M2:  $M1 + M2 \rightarrow M3$



Figure 7-3: Math Equation Editor Configured for the Two-Wattmeter Power Measurement Method.

The three math waveforms M1, M2, and M3 are shown in Fig. 11. Primary interest is in the math waveform M3 which shows the total active power waveform. By computing the mean value of the M3 signal the total active three-phase power value on the output of the drive inverter can be computed. In the example shown below the output power value equates to  $P_{out} = 164.72 W$ .



Figure 7-4: Math Waveforms based on Voltage and Current Measurements on Ch1 - Ch4.

Math waveforms M1, M2 showing the individual power values of each wattmeter and math waveform M3 showing the overall power waveform. The mean values of M3 gives the total active three-phase output power of the drive inverter. In this case  $P_{out} = 164.72 \text{ W}$ .

### 7.1.3 Inverter Efficiency

Finally, the electrical efficiency of the drive inverter can be computed with Equation (1)

$$\eta = \frac{164.72 \text{ W}}{182.85 \text{ W}} = 0.899 = 89.9 \%$$

To verify the efficiency value a computational analysis of the voltage and current waveforms was conducted in MATLAB. In Table 7-1 the measured power values and electrical efficiency are shown for different test conditions. The computed efficiency values in MATLAB based on the captured signals show a good agreement with the measured and computed values of the oscilloscope with an error of < 1%.

Test Condition*	Input Power [W]	Output Power [W]	Efficiency $\eta$ (calculated within Oscilloscope) [%]	Efficiency $\eta$ (Calculated with MATLAB) [%]
30 A, 1250 rpm	182.85	164.72	89.88	90.28
30 A, 1250 rpm**	184.7	168.4	91.17	91.15
30 A, 1750 rpm**	250.7	233.1	93.01	93.07
30 A, 2500 rpm**	350.7	332.1	94.69	94.64

Table 7-1: Electrical Efficiency Values for Different Test Conditions.

\* first value: DC load current of the load motor in A, second value: motor speed in rpm

\*\* measurements conducted in one day with same conditions

## 8 Conclusion

The presented motor test bench and measurement setup was used successfully to evaluate the electrical efficiency of the drive inverter for different load conditions. Generally, any kind of three-phase drive inverter independent of the control method can be tested and evaluated by this setup. In-depth knowledge of the drive inverters electronic architecture is not needed to assess its power efficiency. However, in case the user would like to optimize the drive inverter regarding efficiency, additional voltage and current measurements inside the inverter hardware with the oscilloscope will support this optimization process.

With the proposed measurement concept all voltage and current signals required for the power-efficiency analysis were measured successfully. The power values which were computed by the built-in "Math-function" of the R&S®RTM-3004 oscilloscope have shown good agreement with the results obtained from a computational analysis of the signals in MATLAB. Overall, the two-wattmeter method shows good applicability for the active power measurement of three-phase power systems with 4-channel oscilloscopes. This is not only helpful to save valuable (and costly) inputs on measurement instruments but also reduces the costs of the required laboratory and measurement equipment.

## 9 Literature

- [1] J.R. Hendershot, Timothy John Eastham Miller, Design of Brushless Permanent-Magnet Mashines, Edition 2, Motot Design Books LLC, 2010.
- [2] Institute for Power Electronics and Electrical Drives, RWTH Aachen University, Fang Qi, Daniel Scharfenstein, Claude Weiss, "www.infineon.com," 12 03 2019. [Online]. Available: [https://www.infineon.com/dgdl/Infineon-motorcontrol\\_handbook-AdditionalTechnicalInformation-v01\\_00-EN.pdf](https://www.infineon.com/dgdl/Infineon-motorcontrol_handbook-AdditionalTechnicalInformation-v01_00-EN.pdf). [Accessed 30 01 2021].
- [3] P. Pillay and R. Krishnan, "https://ieeexplore.ieee.org," "Application characteristics of permanent magnet synchronous and brushless DC motors for servo drives," in IEEE Transactions on Industry Applications Sept.-Oct. 1991. [Online]. Available: <https://ieeexplore.ieee.org/document/90357>.
- [4] C. Mistretta and F. Scrimizzi, "https://www.st.com," 11 2018. [Online]. Available: [https://www.st.com/resource/en/application\\_note/dm00560907-lowvoltage-power-mosfet-switching-behavior-and-performance-evaluation-in-motor-control-application-topologies-stmicroelectronics.pdf](https://www.st.com/resource/en/application_note/dm00560907-lowvoltage-power-mosfet-switching-behavior-and-performance-evaluation-in-motor-control-application-topologies-stmicroelectronics.pdf). [Accessed 30 01 2021].
- [5] K. Johnson, "https://teledynelecroy.com," 2017. [Online]. Available: [https://teledynelecroy.com/japan/pdf/motordrive/motor\\_drive\\_technical\\_primer\\_sample.pdf](https://teledynelecroy.com/japan/pdf/motordrive/motor_drive_technical_primer_sample.pdf). [Accessed 30 01 2021].
- [6] Blondel, A., "Measurement of the energy of polyphase currets," International Electrical Congress, Chicago, 1893.
- [7] Considine, Douglas M.; Glenn, D.;, Van Nostand's Scientific Encyclopidia, Springer US, 1995.
- [8] Rohde&Schwarz, "Rohde & Schwarz, "R&S®RT-ZF20 Power Deskew Fixture Manual," 2019.," [Online]. Available: [https://scdn.rohde-schwarz.com/ur/pws/dl\\_downloads/pdm/cl\\_manuals/user\\_manual/1800\\_0040\\_01/RT-ZF20\\_UserManual\\_en\\_05.pdf](https://scdn.rohde-schwarz.com/ur/pws/dl_downloads/pdm/cl_manuals/user_manual/1800_0040_01/RT-ZF20_UserManual_en_05.pdf). [Accessed 30 01 2021].

# 10 Ordering Information

Designation	Type	Order No.
Oscilloscope, 70MHz bandwidth, 4 channels	R&S®RTM3004	1335.8794.04
Differential High Voltage Probe	R&S®RT-ZHD07	1800.2307.02
Current Probe	R&S®RT-ZC10B	1409.8210.02
Power Supply	R&S®NGP814	5601.4007.04

## Rohde & Schwarz

The Rohde & Schwarz electronics group offers innovative solutions in the following business fields: test and measurement, broadcast and media, secure communications, cybersecurity, monitoring and network testing. Founded more than 80 years ago, the independent company which is headquartered in Munich, Germany, has an extensive sales and service network with locations in more than 70 countries.

[www.rohde-schwarz.com](http://www.rohde-schwarz.com)



## Rohde & Schwarz training

[www.training.rohde-schwarz.com](http://www.training.rohde-schwarz.com)

## Rohde & Schwarz customer support

[www.rohde-schwarz.com/support](http://www.rohde-schwarz.com/support)



R&S® is a registered trademark of Rohde & Schwarz GmbH & Co. KG  
Trade names are trademarks of the owners.

GFM360 | Version 0e | 04.2021

Application Note | Efficiency Measurement of a 3-Phase Inverter for a BLDC Motor

Data without tolerance limits is not binding | Subject to change

© 2021 Rohde & Schwarz GmbH & Co. KG | 81671 Munich, Germany

[www.rohde-schwarz.com](http://www.rohde-schwarz.com)